Note

A novel solution reaction of hexahydridoferrate(4−) with iron(II) that produces iron particles

Donald E. Linn Jr. [a,*], Yisong Guo [b], Stephen P. Cramer [b]

[a] *Department of Chemistry, Indiana University Purdue University Fort Wayne, Fort Wayne, IN 46805, United States*
[b] *Department of Applied Science, University of California, Davis, CA 95616, United States*

Abstract

This report is the description of a reaction that produces iron(0) from the room temperature reaction in THF solution between $[MgX(THF)_2]_4[FeH_6]$ (X = Cl and Br) and $FeCl_2$. The production of α-iron is demonstrated by powder XRD and Mössbauer spectroscopy. The lattice spacings (d), isomer shift (δ), nuclear quadrupole (ΔE_Q), and magnetic hyperfine (H_{hf}) parameters determine that the material consists of the bcc phase of iron.
© 2007 Elsevier B.V. All rights reserved.

Keywords: Homoleptic hydride; Iron particle; Synproportionation (comproportionation) reaction

1. Introduction

Metallic iron can be readily prepared by a variety of solution techniques that include: (1) expulsion of CO from pentacarbonyliron(0) [1]; (2) reduction of iron halides in aqueous solutions of borohydride [2], (3) or in nonaqueous solutions using alkylborohydrides [3], aluminum alkyls [4], transition metal organometals [5] and electrides [6]; and, high-temperature hydrogenation of iron oxygen species [7]. Reactions that form iron particles in solution using $Fe(CO)_5$ are known to follow a complex pathway [8].

The presence of a potentially oxidizing or a strong ligand such as water and CO, respectively, makes the preparation of systems approaching "naked iron" difficult. Such compositions would be potentially useful. Amorphous and nanoparticulate iron species have been studied extensively for their catalytic [9], magnetic [10], and biomedical uses [11].

Homoleptic complex hydrides unlike metal carbonyls contain no traditional acceptor orbitals (e.g. π-acceptors)

that would favor the formation of the zero-valent oxidation state in metals. The ability of the hydride ligand to support lower oxidation states has suggested $[MgX(THF)_2]_4[FeH_6]$ (X = Cl and Br) as a precursor in the synthesis of iron materials. The reaction chemistry of the homoleptic transition metal hydrides has escaped attention mostly, and to date the known soluble homoleptic transition metal hydride complexes encompass only $[MH_6]^{4-}$ (M = Fe and Ru) and $[MH_9]^{2-}$ (M = Tc and Re) [12]. An iron deposition reaction that utilizes the soluble homoleptic iron hydride complex, $[FeH_6]^{4-}$, would represent a novel approach.
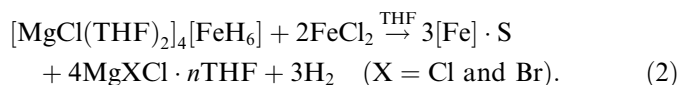
Our previous results had shown that addition of alcohol (water) results in oxidation of $[FeH_6]^{4-}$:

$$[FeH_6]^{4-} + 6ROH \rightarrow [Fe]^{2+} + 6RO^- + 6H_2 \qquad (1)$$
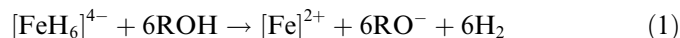
(R = alkyl, H).

An H_2 evolving reaction that utilizes water at neutral pH would require a modest thermodynamic potential (−0.41 V versus NHE) similar to the Fe^{2+}/Fe half-reaction (−0.44 V versus NHE) [13]. Coupling the reduction of a transition metal halide such as iron(II) halide and concomitant oxidation of $[FeH_6]^{4-}$ might be written:

* Corresponding author. Tel.: +1 260 481 6813; fax: +1 260 481 6070.
E-mail address: linn@ipfw.edu (D.E. Linn Jr.).

$$[MgCl(THF)_2]_4[FeH_6] + 2FeCl_2 \overset{THF}{\rightarrow} 3[Fe] \cdot S$$
$$+ 4MgXCl \cdot nTHF + 3H_2 \quad (X = Cl \text{ and } Br). \quad (2)$$

In THF solution it might be anticipated that the reactions would be modulated due to the effects of ion pairing, to make such a process uncertain. We now report our findings to substantiate this reaction.

2. Experimental

The complex hydride, $[MgCl(THF)_2]_4[FeH_6]$ (X = Cl and Br), was prepared and handled as were other reagents as described previously [14].

In one case synthesis of iron in reaction (2) (X = Cl) consisted of preparing a solution of 0.264 g (0.300 mmol) $[MgCl(THF)_2]_4[FeH_6]$ in 50 mL THF and adding 0.076 g (0.60 mmol) $FeCl_2$ and stirring overnight at room temperature. A Fe-57 enriched sample was also prepared analogously with $^{57}FeCl_2$.

Analysis of iron was performed by digesting each sample in sulfuric acid and forming the $[Fe(phen)_3]^{2+}$ complex which was determined spectrophotometrically at 508 nm [15]. Further, magnesium analysis was determined using ETDA titrations with Eriochrome-T as the indicator and chloride where X = Cl was determined by $AgNO_3$ titrations with K_2CrO_4 as the indicator (Mohr method) [15]. Otherwise, combustion analyses (CHN), magnesium and halide analyses, where X = Br were performed by the Microanalytical Laboratory, Purdue University, West Lafayette.

Diffraction patterns were obtained using a PANalytical X'Pert PRO MPD X-ray diffraction system (PANalytical, Almelo, The Netherlands) equipped with a PW3050/60 θ–θ goniometer and a Co-target X-ray tube operated at 40 keV and 35 mA ($\lambda = 1.790307$ Å). Incident beam optics consisted of an Fe beta filter, 0.04 radian Soller slit, a programmable divergence slit, and a beam mask set to illuminate a 15×15 mm sample area. The diffracted beam optics consisted of a programmable diffracted beam anti-scatter slit, a 0.04 radian Soller slit, and a PW3015/20 X'Celerator detector configured for an active length of $2.122°$ 2θ. The sample was mounted on a glass slide and covered with 6 µm thick Myar tape. The sample was scanned from at $0.033°$ steps with 60 s measurement time per step. The data were analyzed with the X'Pert High Score Plus software package and were converted to a fixed $1°$ divergence slit prior to phase analysis and plotting.

The Mössbauer spectra, Fig. 2, were recorded at 78 K using conventional sine-wave-acceleration spectrometer with Oxford OptistatDN cryostat. The sample was sealed in a nitrogen-filled glass vial after synthesis and shipped to the University of California, Davis. The Mössbauer absorber then was prepared in a pure dry nitrogen gas glovebox by mixing the sample with deoxygenated boron nitride to form finely dispersed material. The spectrometer includes a Wissel 1200 Mössbauer velocity drive and a
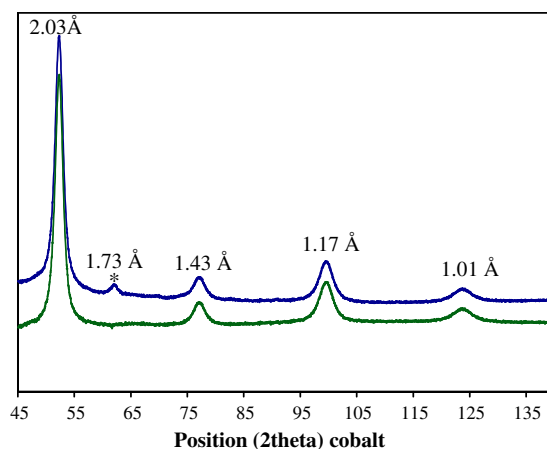

Fig. 1. XRD pattern (upper trace) of intensity vs. position of sample sealed with a Mylar barrier over glass. The lower trace of blank Mylar over glass subtracted from the upper trace offset to show a 1.73 Å artifact. Intense low angle reflections are outside the region of interest.

LND-45431 proportional counter, and a room-temperature rhodium-matrix cobalt-57 source, which was calibrated at room temperature with 25 µm α-iron foil. The sample measurement was conducted at liquid nitrogen temperature to avoid exposure to oxygen.

3. Results and discussion

Performing reaction (2) above resulted in a pyrophoric black solid, $[Fe] \cdot S$, (see Section 2 and Table 1, Supporting Information).[1] The solution was stirred overnight and the product collected on a magnetic stir bar (see Fig. 1S, Supplementary Information), washed with THF and dried to obtain quantitatively iron (98%). The composition of the iron product was typically 83–86% iron. Evaporation of the solvent yielded the magnesium halide by-product, e.g. $MgCl_2 \cdot nTHF$ (0.187 g, n = 1.25, see Table 1, Supporting Information) isolated in 84–90%.

A powder XRD (Fig. 1) shows broad peaks that match the pattern in the JCPDS standard 06-696, that corresponds to single phase, bcc iron with reported lattice d spacings (Miller indices, relative intensity) of 2.03 (1 1 0, 100), 1.43 (2 0 0, 10), and 1.17 (2 1 1, 20), 1.01 Å (2 2 0, 5) [16].

A Mössbauer spectrum of ^{57}Fe-labeled product from reaction (2) is illustrated in Fig. 2. The hyperfine field distribution was generated to fit the pattern by using the histogram and maximum entropy methods as options in the data refinement [17]. The fitting indicates that the material is in the α-iron phase where the line broadening of Mössbauer spectrum may be due to the heterogeneity of the material, which causes a distribution of hyperfine fields [18]. This is consistent with the broad bcc iron peaks in the powder X-ray diffraction pattern. Data refinement using a results in an isomer shift (δ), nuclear quadrupole

---

[1] The iron species synthesized in these reactions are formulated as [Fe]·S. This indicates the presence of surface substrates: MgX_2 and THF are confirmed by the analytical data (see Table 1, Supporting Information).
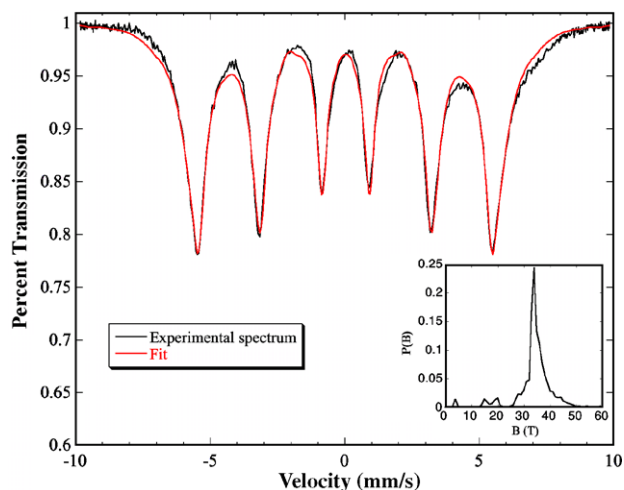
Fig. 2. Mössbauer spectrum of iron sample from reaction (2) prepared using $^{57}FeCl_2$ at 78 K (black solid line) and simulation (red solid line). Inset shows the magnetic hyperfine field distribution profile from 0 to 60 Tesla obtained from NORMOS-90 simulation. (see Supporting Information, Table 2 for Mössbauer parameters). (For interpretation of the references in colour in this figure legend, the reader is referred to the web version of this article.)

(ΔE_Q), and magnetic hyperfine ($\langle H_{hf} \rangle$) (see data refinement Table 2, Supporting Information).

The conversion obtained in reaction (2) between $[FeH_6]^{4-}$ and $[Fe^{II}]$. might be considered a novel example of synproportionation (comproportionation). Further, the present reaction concerns the ability of hydrogen to bind to a metal center and undergo reductive elimination [19]. Here, once oxidized, a proton from the resulting metal complex can transfer to a bound hydride to form the H_2 ligand. Molecular hydrogen can be expelled readily, in this case, to produce ultimately elemental iron.

4. Conclusions

To summarize, a mild solution reaction has been developed to produce iron particles supported only by solvated magnesium halide. These metallic iron particles are produced solely in the α-phase as deduced by XRD, and Mössbauer spectroscopy. Further work intends to pursue the mechanism for the reaction, its generality, and the scope of materials comprised of iron accessible by this technique.

Acknowledgements

Appendix A. Supplementary material

Supplementary data associated with this article can be found, in the online version, at doi:10.1016/j.ica.2007.09.032.

References

[1] D. Farrell, S.A. Majetich, J.P. Wilcoxon, J. Phys. Chem. 107 (2003) 11022, and references therein.

[2] S.-J. Cho, A.M. Shashin, G.J. Long, J.E. Davies, K. Lau, F. Grandjean, S.M. Kauzlarich, Chem. Mater. 18 (2006) 960, and references therein.

[3] H. Bönnemann, G. Braun, W. Brijoux, R. Brinkman, A. Schulze Tilling, K. Seevogel, K. Siepen, J. Organomet. Chem. 520 (1996) 143; Z. Guo, L.L. Henry, V. Palshin, E.J. Podlaha, J. Mater. Chem. 16 (2006) 1772.

[4] M. Antonietti, L. Wenz, L. Bronstein, M. Seregina, Adv. Mater. 7 (1995) 1000.

[5] R. Choukroun, D. de Caro, S. Mantéo, C. Amiens, B. Chaudret, E. Snoeck, M. Respaud, New J. Chem. 22 (1998) 1295.

[6] K. Tsai, J.L. Dye, J. Am. Chem. Soc. 113 (1993) 1650.

[7] C. Gong, D. Chen, X. Jiao, Q. Wang, J. Mater. Chem. 12 (2002) 1844.

[8] M. Zubris, R.B. King, H. Garmestani, R. Tannenbaum, J. Mater. Chem. 15 (2005) 1277.

[9] H. Bönnemann, R.M. Richards, Eur. J. Inorg. Chem. 10 (2001) 2455.

[10] S.C. Sun, C.B. Murray, L.F. Weller, M. Andreas, Science 287 (2000) 1989, and references therein.

[11] J.K. Vasir, M.K. Reddy, V.D. Labhassetwar, Curr. Nanosci. 1 (2005) 47.

[12] R.B. King, Coord. Chem. Rev. 200–202 (2000) 813.

[13] A.J. Bard, R. Parsons, J. Jordon (Eds.), Standard Reduction Potentials in Aqueous Solutions, Marcel Dekker Inc., New York, NY, 1985.

[14] D.E. Linn Jr., G.M. Skidd, S.N. McVay, Inorg. Chem. 41 (2002) 5320.

[15] D.A. Skoog, D.M. West, F.J. Holler, Fundamentals of Analytical Chemistry, third ed., in: W.B. Saunders (Ed.), Philadelphia, 1996 (see pp. 859, 831, 829, respectively).

[16] Joint Committee for Powder Diffraction Standards, The Mineral Powder Diffraction File (JCPDS); International Center for Diffraction Data: Swarthmore, Pennsylvania, 1967.

[17] R.A. Brand, NORMOS-90 Mössbauer Fitting Program Package, Wissenschaftliche Elektronik GmbH, Starnberg, Germany.

[18] M. Maillard, L. Motte, A.T. Ngo, M.P.J. Pileni, Chem. Phys. B 104 (2000) 11871.

[19] G. Kubas, Proc. Natl. Acad. Sci. USA 104 (2007) 6901.